

# Wireless sensor network for determining boat motions and hydroelastic responses.

Denchfield, S., Winden, B., Brooks, C.J., Turnock, S.R., Hudson, D.A., Forrester, A.I.J., Taunton, D.J.

*School of Engineering Sciences, University of Southampton, Southampton SO17 1BJ, UK*

## Abstract

A flexible segmented ship model has been tested in a series of head sea wave conditions including regular, irregular and a rogue wave. The model has a typical frigate form and is constructed using a flexible central spine against which four segments are mounted. A three node wireless sensor system, which currently acquires data at up to 30Hz was also attached to the model. These wireless development sensors were supplied as part of the ESPRIT programme and incorporate 9 degrees of freedom using rotational and translational accelerometers and a 3 component magnetometer. The data acquired was compared to those obtained using the traditional pitch and heave potentiometers and a standard heave accelerometer. Overall, the system, although still requiring further development to improve data acquisition rate, performed well with good correlation observed between the various measurement components. The practical advantages are the low mass and low power requirements of such a wireless sensor network.

## 1. Introduction

The accurate capture of free running model ship motion tests requires a data acquisition system that is sufficiently low mass that installation will not alter the behaviour of the model to the seaway as well as being able to record data of sufficient quality for the test duration, see for example the tests of Molland *et al* (2001). The recent rapid reduction in costs of low power low mass sensor systems primarily driven by production scale applications such as car airbags, mobile phones and game consoles allows access to measurement technology at a greatly reduced cost. However, there is still a question as to whether the measurements can be made at a sufficient level of absolute accuracy to be of use to the hydrodynamicist. In all the previous applications relative measurements are usually sufficient.

A large scale research programme (ESPRIT <http://vip.doc.ic.ac.uk/esprit/m780.html>), funded by the UK's Engineering and Physical Sciences Research council is investigating the application of wireless sensor technologies to sport. Through this programme the University of Southampton is carrying out a proof of concept study into the application of wireless sensors for various marine sports. As part of this study a comparative set of tests have been carried out to assess the measurement quality of a network of three sensors mounted on a ship model whose response to a variety of seastates is already known (Denchfield, 2011).

## 2. Ship Model

A flexible model of a Leander class frigate, with the principal particulars in Table 1, was constructed at a scale of 1:43.62. The hull, shown in Figure 1, consisted of four rigid segments attached to a uniform flexible aluminium backbone designed to match the dry natural frequency of the first (2-node) bending mode.

**Table 1: Principal particulars of Leander class frigate (model scale)**

Length overall, $L_{OA}$ (m)	2.60
Length between perpendiculars, $L_{BP}$ (m)	2.52
Beam, $B$ (m)	0.29
Draught, $T$ (m)	0.096
Displacement, $\Delta$ (Kg)	29.4
LCG aft amidships (m)	0.091
Service speed, $V$ (m/s)	1.4
Pitch gyradius, $k_{\gamma\gamma}$ (% $L_{OA}$ )	17.11
2-node natural frequency, $\omega_n$ (rad/s)	94.3



**Figure 1: The flexible model hull installed in the towing tank**

## 3. Test Programme

Experiments were carried out in the Southampton Solent University unidirectional towing tank, 60m in length, 3.7m in breadth and 1.86m in depth.

All testing was carried out at the ship service speed of 1.4m/s, corresponding to 18 knots full scale. Preliminary experiments were carried out in regular waves, at a steepness of 0.02. Tests were then undertaken in irregular seas – one random and two containing a rogue wave. Rogue waves were modelled first using the NewWave technique of Tromans et al (1991), and secondly using an optimisation process based on the technique of Clauss and Steinhagen (2000). These techniques have previously been applied to testing of rigid body motions in Denchfield et al (2010). Each of the irregular seas was modelled using a JONSWAP spectrum with a significant wave height of 100mm, a peak wave

period of 1.45s and a  $\gamma$  of 3.3 The rogue wave height where applicable was 236mm and in each case was encountered at midships.

Measurements were taken of heave and pitch. The wireless sensors were installed on the flexible beam at the forward and aft ends, and the longitudinal centre of gravity of the model. In addition a conventional (wired) accelerometer capable of measuring vertical accelerations was installed at the longitudinal centre of gravity in order verify the results obtained from the wireless sensors.

#### 4. Response in regular waves

An example 5 second segment of a recorded wave profile, heave, pitch and vertical accelerations (recorded using the conventional wired accelerometer) is given in Figure 2 for an example wave frequency of 3.93rad/s (hence encounter frequency of 6.13rad/s) and a wave height of 87mm. Figure 3 compares heave and pitch RAOs to those obtained previously for the model hull (Denchfield, 2011). In addition, results from a 2D linear hydroelasticity analysis (previously presented in Denchfield et al, 2010) are shown. Good agreement is seen between the different results.

Figure 4 shows the vertical acceleration RAO at midships obtained from the conventional wired accelerometer.

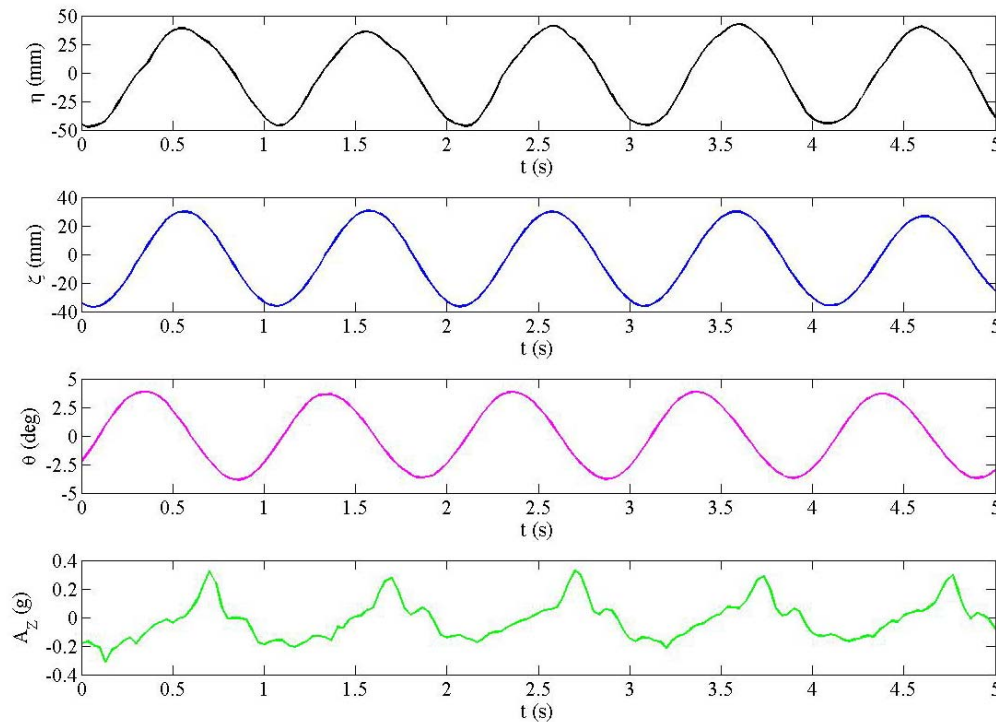


**Figure 2: Recorded regular wave profile, heave, pitch and vertical acceleration (using a conventional accelerometer) in a wave with a frequency of 3.93rad/s and height of 87mm, at 1.4m/s**

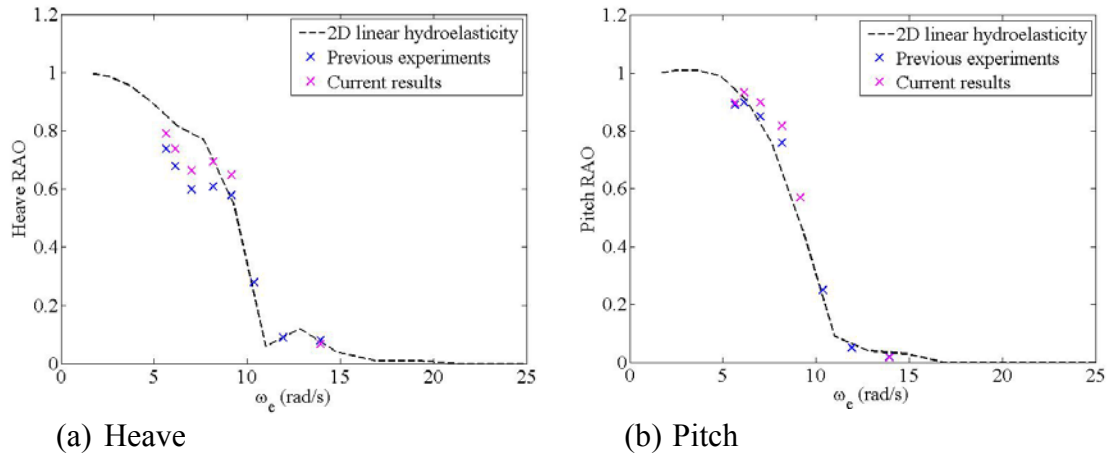


Figure 3: Response Amplitude Operators (RAO) for model in regular waves at 1.4m/s

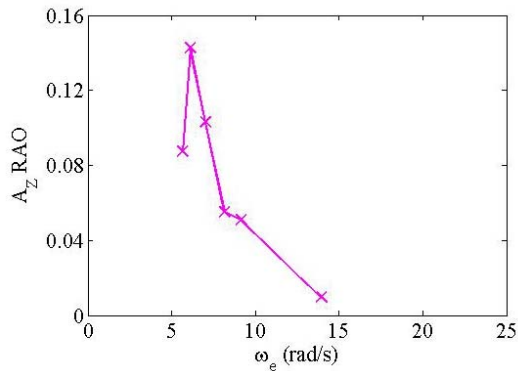
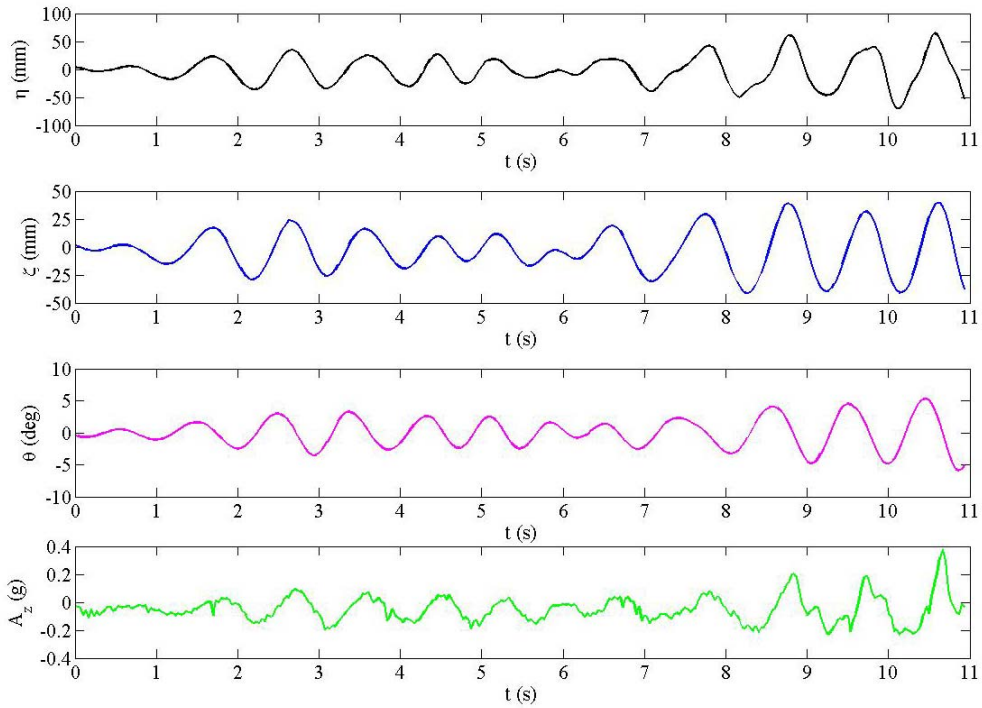


Figure 4: Vertical acceleration RAO obtained from conventional accelerometer in regular waves at 1.4m/s, at midships

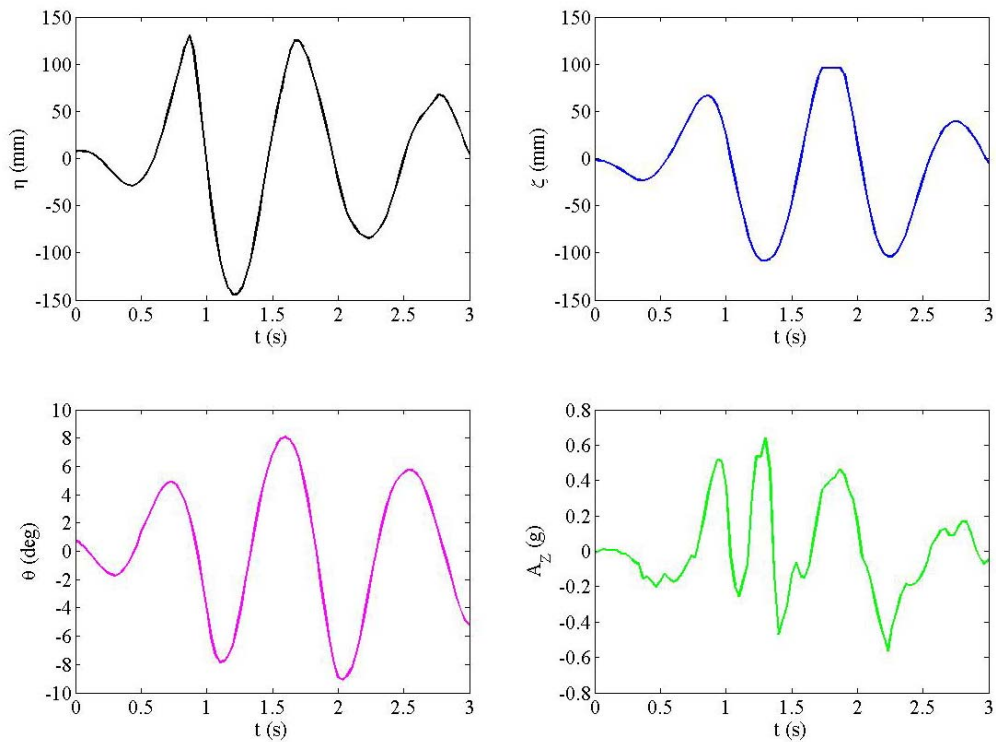
## 5. Response in rogue waves

Figure 5 shows the recorded wave profile, heave, pitch and vertical acceleration (using the wired accelerometer) in the random sea with the ship travelling at 1.4m/s; the equivalent for the NewWave and optimised seas are in Figure 6 and Figure 7. Table 2 gives details of maximum (trough to crest) wave height, heave, pitch and vertical acceleration recorded in each sea.

Some water ingress occurred during experiments, affecting the data acquisition. This is particularly visible in the vertical acceleration data in the optimised sea (Figure 7), and is also responsible for the sharp reduction in vertical acceleration at 1.1s in the NewWave sea (Figure 6). Note also that the heave measurement topped out in the NewWave sea.



**Figure 5: Wave profile and heave, pitch and vertical acceleration measurements in a random JONSWAP sea with a significant wave height of 100mm at 1.4m/s**



**Figure 6: Wave profile and heave, pitch and vertical acceleration measurements in a NewWave sea with a significant wave height of 100mm, at 1.4m/s**

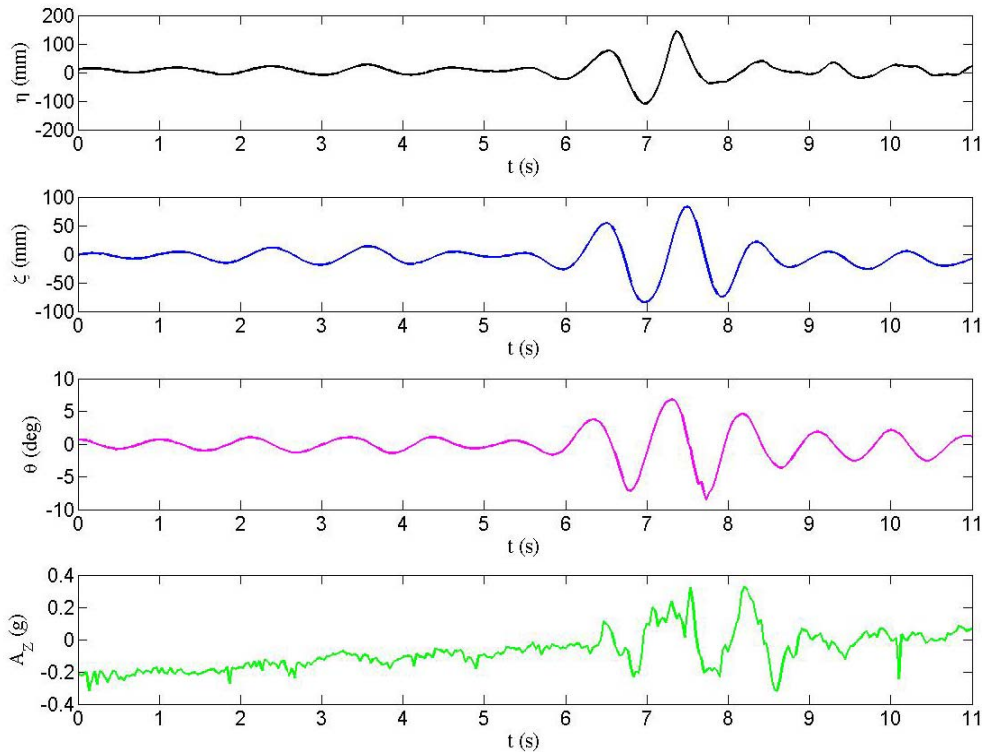


Figure 7: Wave profile and heave, pitch and vertical acceleration measurements in an optimised sea with a significant wave height of 100mm, at 1.4m/s

Table 2: Maximum (trough to crest) wave height ( $\eta_{MAX}$ ), heave ( $\zeta_{MAX}$ ), pitch ( $\theta_{MAX}$ ) and vertical acceleration from the conventional accelerometer ( $Az_{MAX}$ ) recorded in each sea state

SEA STATE	$\eta_{MAX}$ (mm)	$\zeta_{MAX}$ (mm)	$\theta_{MAX}$ (deg)	$Az_{MAX}$ (g)
Random	134.36	80.34	11.17	0.605
NewWave	274.40	204.44	17.13	1.110
Optimised	253.10	167.30	15.35	0.642

As expected the rogue seas produce more severe motions than the random sea, although in the case of vertical acceleration it is only by a small amount in the optimised sea. This is likely to be due to the water ingress into the data acquisition affecting the results. The severity of the rogue wave influence can be further seen through images recorded through the use of a waterproof camera mounted 91cm from the bow of the model and 16cm above the deck level. These are shown in Figure 8.



Figure 8: Rogue wave encounter at 1.4m/s showing the rogue wave approaching, bow immersion and recovery phases.

## 6. Comparison with wireless sensor performance

Three Magnetic, Angular Rate, and Gravity (MARG) sensor units were positioned on the ship model. Each sensor unit consists of a three-axis accelerometer, a three-axis magnetometer, and a three-axis gyroscope. These provide data for three mutually orthogonal axes, which can be used, in conjunction with a suitable orientation filter, to provide a complete measurement of orientation. The motes themselves, Figure 8, consist of a battery board, a CPU board (with microcontroller, RF transceiver, flash memory and LEDs), and sensor board containing the MARG sensors. A 'basestation' CPU board, in conjunction with a USB programming board, enables communication with the motes, providing a serial connection for downloading or streaming data to a PC. The motes are run on the TinyOS operating system, and data is either streamed wirelessly to the PC, or logged on the 4Mb onboard flash storage.

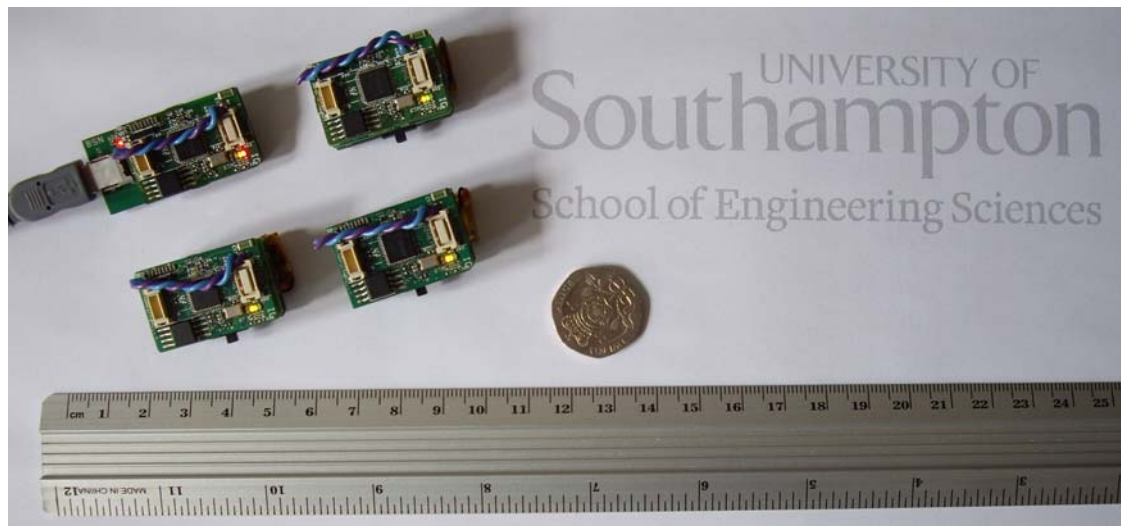


Figure 8: MARG sensor units used are Body Sensor Network (BSN) motes supplied by Imperial College London.

### 6.1 Sensor Performance and calibration

The sensor data is received from the motes in un-calibrated decimal format. The accelerometer and magnetometer were calibrated using the 3D ellipsoid method (see Merayo et al. 2000), implemented with a non-iterative algorithm based on a singular value decomposition. The method provides a set of nine coefficients consisting of three offsets, three sensitivities and three non-orthogonal angles, which fully describe each sensor. The calibration procedure consists of a static measurement, from which the gyroscope offsets were obtained, followed by a rotational measurement where the mote is rotated slowly about its origin, and in a fashion which captures as completely as possible the 3D space. Capturing sufficient data usually involves rotating the mote for around two to three minutes. An example of the accelerometer calibration rotational measurement is shown in Figure 9, where the square root of the sum of squares of the physical components is plotted, in addition to the calibrated data for each component.

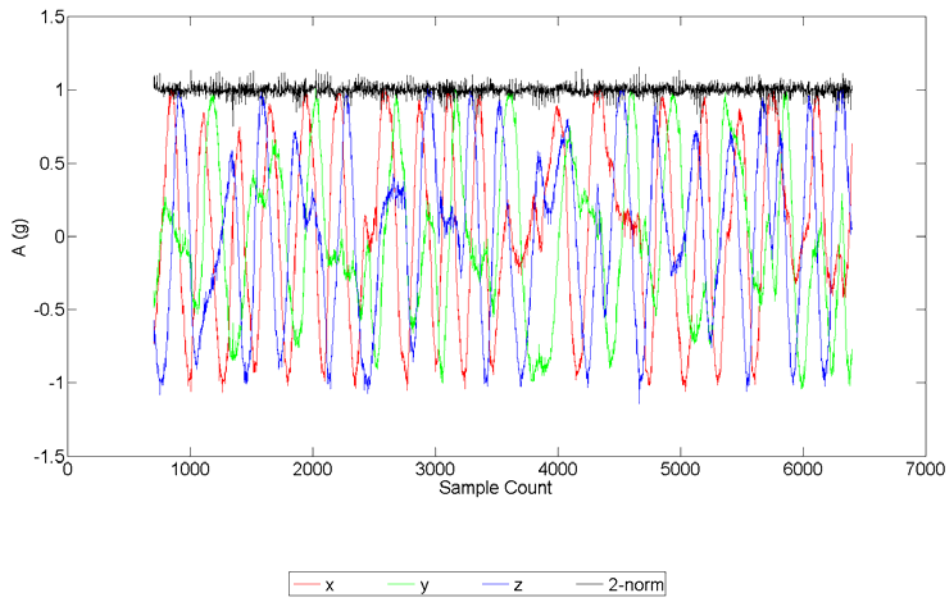


Figure 9. Example of accelerometer calibration rotational measurement, displaying calibrated components and the resulting 2-norm.

## 6.2 Sensor application

The orientation of the wireless motes relative to the Earth-fixed frame can be estimated by fusing the accelerometer, magnetometer and gyroscope signals via filtering methods. A large body of work exists for such filters, primarily developed for aerospace (Crassidis et al. 2007), robotics (Vaganay et al. 1993), control (Zimmerman & Sulzer 1991) and human body motion (Marins et al. 2001) applications. In the present work, a quaternion-based complementary filter is implemented, based on the Direction Cosine Matrix (DCM) filter of Mahony, R. et al. (2008), and containing the magnetic distortion compensation method of Madgwick, S. O. H. et al. (2010). An example of the filter output is shown in Figure 10, with and without the magnetometer data, for a sequence of approximate 90 degree rotations about each axis performed by hand.

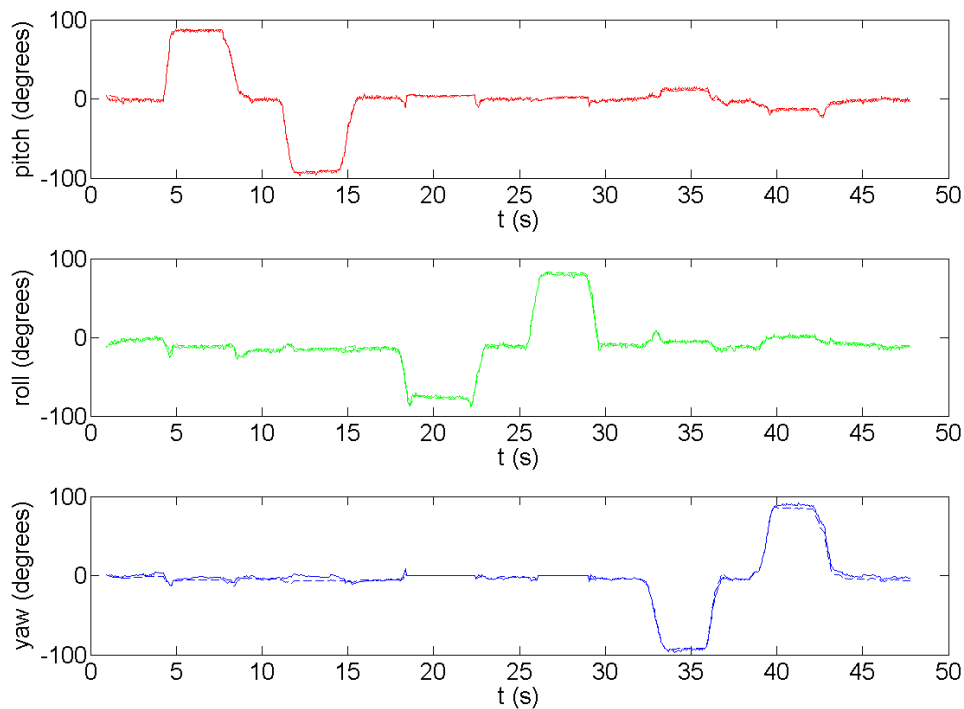
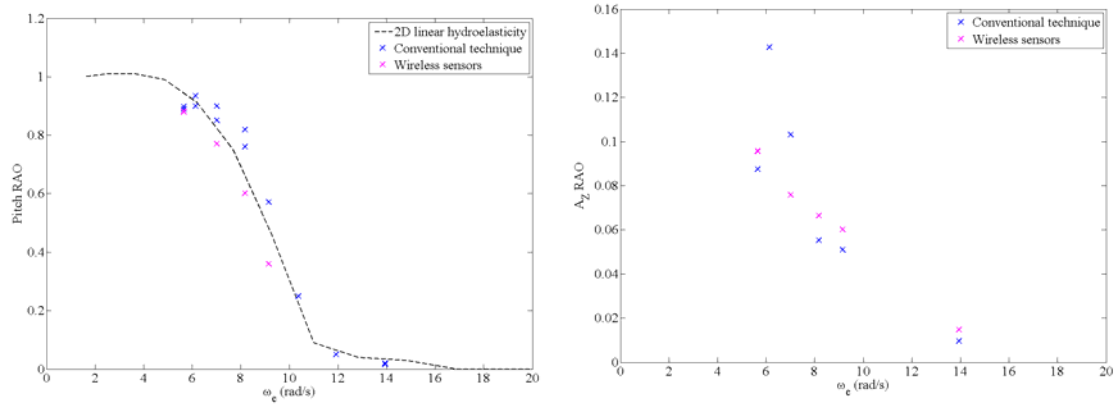


Figure 10 Example of complementary filter Euler angle output for a sequence of approximate 90 degree rotations performed statically, by hand. Solid line is the output from MARG filter and dashed line is the output from IMU filter.

During the present experiments the magnetometer data was not recorded, therefore there was no absolute reference of yaw. However, since the heading of the flexible hull model was fixed in the experiments, the effect on the determined pitch and roll angles is negligible.

### 6.3 Regular sea results

Figure 11 presents regular wave RAOs for pitch and vertical acceleration obtained using the wireless sensors at midships, in comparison to results obtained using conventional techniques (i.e a wired accelerometer at midships to obtain vertical acceleration, and pitch measurements using a potentiometer). The pitch response obtained from the wireless sensors was calculated from the acceleration data using Equation 1. An example of the acceleration data in the x, y and z directions and the obtained pitch data is given in Figure 10 for a regular wave with a frequency of  $4.33\text{rad/s}$  and a height of  $70.23\text{mm}$ . The results obtained from the wireless sensors were filtered using a low-pass filter in order to remove high frequency noise. In the cases of the z-acceleration and the pitch response, the data obtained using the described conventional techniques is also shown. Good agreement is seen in the RAOs in Figure 11 between results obtained using the wireless sensors, and those from more conventional techniques, with the main difference in vertical accelerations being the more sinusoidal nature of the results obtained from the wireless sensors compared to the conventional wired accelerometer. One potential reason for this may have been the sample rate of the accelerometer and sensors, but further investigation is required.



(a) Pitch (b) Heave  
**Figure 11: Pitch and Vertical acceleration RAOs at midships obtained from the wireless sensors in comparison to results from conventional methods, at 1.4m/s in regular waves.**

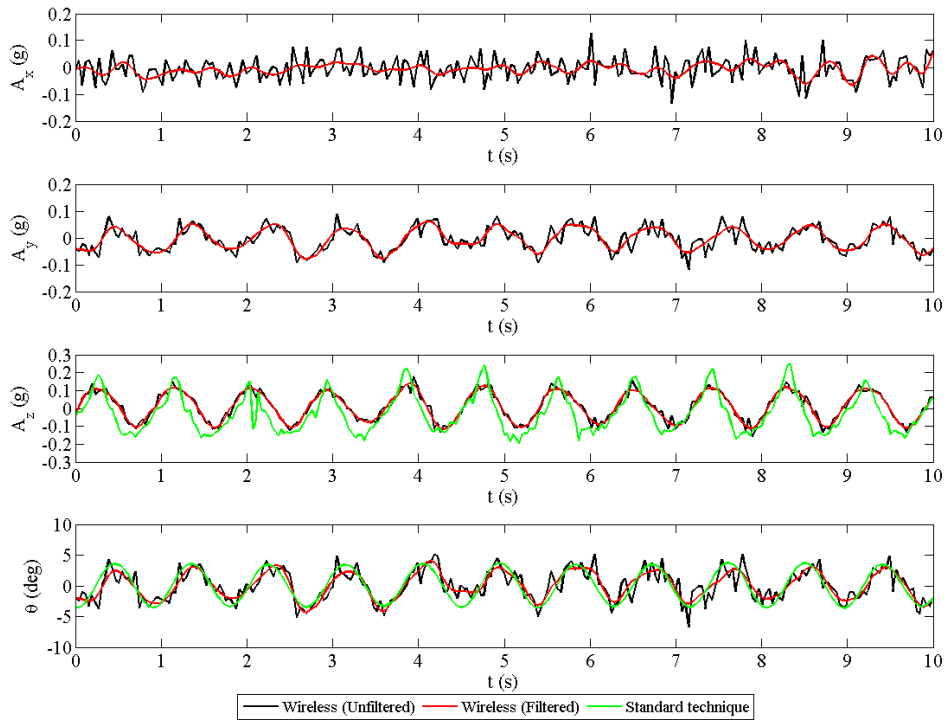


**Figure 12: Demonstration of acceleration data obtained for the x, y and z directions at midships, and the calculated pitch, in comparison to results using conventional techniques. Results are for a regular wave with a frequency of 4.33rad/s and a height of 70.23mm at 1.4m/s**

$$\theta = \tan^{-1} \left( \frac{A_x}{\sqrt{A_y^2 + A_z^2}} \right) \quad (1)$$

## 6.4 Rogue sea results

Figure 13 presents the wave profile, heave, pitch and vertical acceleration results obtained using conventional methods (potentiometers for heave and pitch, and a wired accelerometer) in the random sea, along with the pitch, and vertical accelerations at forward, aft and midships locations obtained using the wireless sensors. The equivalent results for the optimised sea are in Figure 14.

It can be seen that there is good agreement between the results obtained using conventional methods and those from the wireless sensors in both the random and rogue seas. Furthermore it is interesting to note that the accelerations recorded at the forward and aft sensors are at least twice those experienced at midships. This is further demonstrated in Table 3 which provides the maximum vertical acceleration values at each location, and the maximum pitch, obtained using the wireless sensors in the random, NewWave and optimised seas.

Although there is no standard technique data for comparison of  $A_Z$  (FWD) and  $A_Z$  (AFT), it can be seen that the sensor data is suitably out of phase, with maxima and minima aligned with the pitch trace.

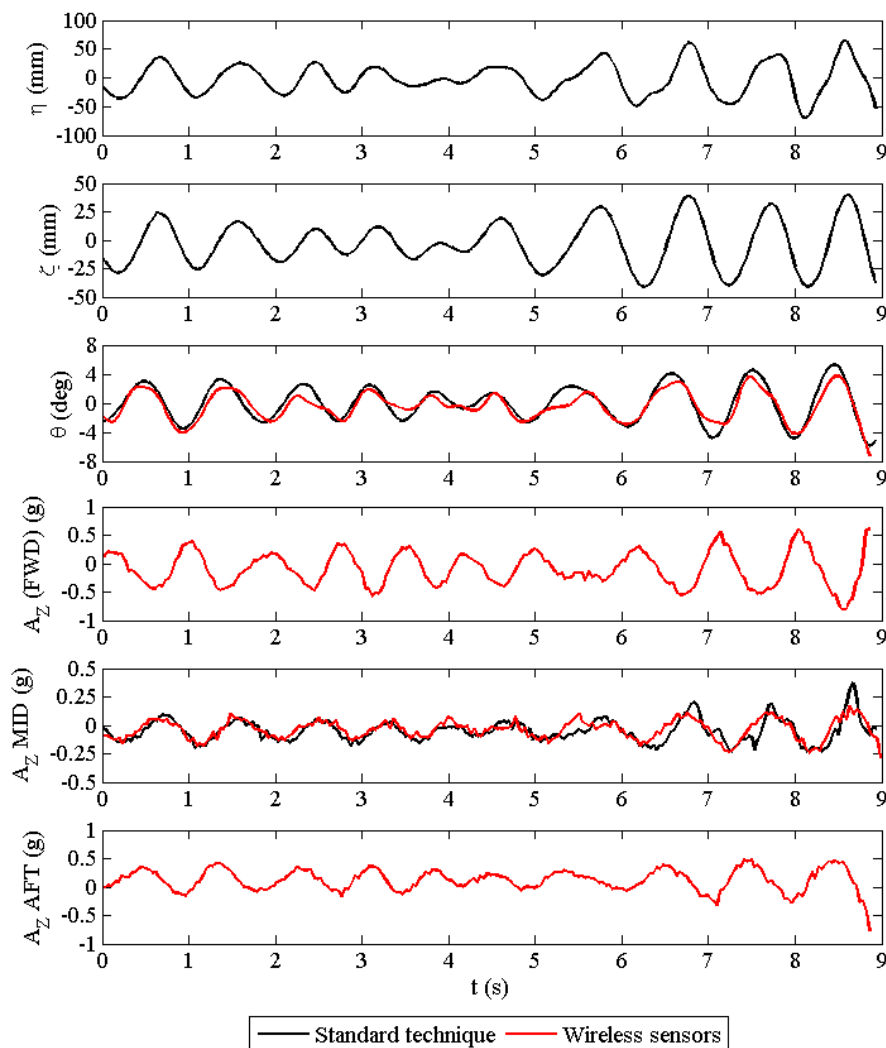


Figure 13: Wave profile, heave, pitch and vertical acceleration measurements obtained through conventional methods and from the wireless sensors, in a random sea at 1.4m/s

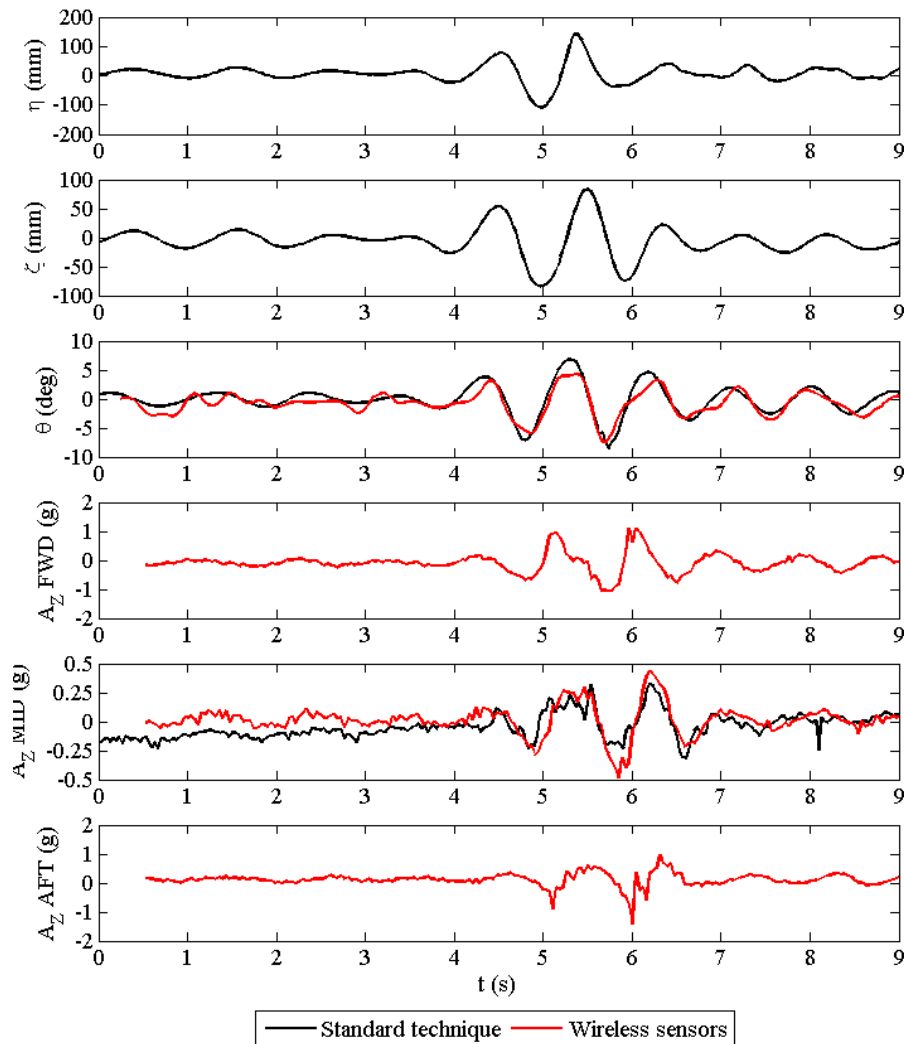


Figure 14: Wave profile, heave, pitch and vertical acceleration measurements obtained through conventional methods and from the wireless sensors, in an optimised sea at 1.4m/s

Table 3: Maximum (trough to crest) pitch ( $\theta_{MAX}$ ) and vertical accelerations ( $A_{Z_{MAX}}$  FWD, MID and AFT) recorded in each sea state using the wireless accelerometers

SEA STATE	$\theta_{MAX}$ (deg)	$A_{Z_{MAX}}$ (g) FWD	$A_{Z_{MAX}}$ (g) MID	$A_{Z_{MAX}}$ (g) AFT
Random	7.92	1.41	0.41	0.75
NewWave	16.89	2.87	1.20	2.40
Optimised	11.61	2.16	0.93	2.37

Looking at the results in Table 3 for pitch and vertical acceleration at midships, in comparison to those obtained using conventional methods (presented in Table 2) it appears that the wireless sensors are able to produce accurate measurements of the responses of a vessel moving in random and rogue seas.

## 7. Conclusions

The rapid reduction in cost of wireless sensor networks will offer many practical benefits for use in hydrodynamics testing provided the sensor data can be acquired at sufficient rate and with reliable and well understood measurement uncertainty. This investigation has shown that such systems can be made robust enough to use.

Overall, the system, although still requiring further development to improve data acquisition rate, performed well with good correlation observed between the various measurement components. The practical advantages are the low mass and low power requirements of such a wireless sensor network.

It is also worth noting that the waterproof video camera mounted near the model bow is an independent unit that records a video stream onto its own memory for subsequent download.

## Acknowledgements

The support provided by the School of Engineering Sciences and Lloyd's Register Educational Trust in funding the PhD studentships of Denchfield, Winden as well as the sensors supplied by Imperial College funded through the ESPRIT programme are gratefully acknowledged.

## References

- Clauss, G. F., and Steinhagen, U., "Optimisation of transient design waves in random sea," Proceedings of 10<sup>th</sup> International Offshore and Polar Engineering Conference, vol. 3, 2000, pp. 229-236.
- Crassidis, J. L., Markley, F. L. and Cheng, Y. (2007) Nonlinear attitude filtering methods. *J. Guidance Control Dynam.*, 30, 1, 12-28.
- Denchfield, S. S., Hudson, D. A., and Temarel, P., "Numerical and experimental evaluation of rogue waves and corresponding ship motions at forward speed," Proceedings of 28<sup>th</sup> Symposium on Naval Hydrodynamics, 2010.
- Denchfield, S. S., "An investigation of the influence of rogue waves on a travelling ship," PhD thesis (submitted), University of Southampton, UK, 2011
- Madgwick, S. O. H. (2010) An efficient orientation filter for inertial and inertial/magnetic sensor arrays. Internal Report, University of Bristol.
- Mahony, R., Hamel, T. and Pflimlin, J.-P. (2008) Nonlinear complimentary filters on the special orthogonal group. *IEEE Trans. Automatic Control*, 53, 5, 1203-1218.
- Marins, J. L., Yun, X., Bachmann, E. R., McGhee, R. B. and Zyda, M. J. (2001) An extended Kalman filter for quaternion-based orientation estimation using MARG sensors. *Proc. IEEE/RSJ Int. Conf. Intelligent Robots and Systems*, Maui, USA.

Merayo, J. M. G., Brauer, P., Primdahl, F., Petersen, J. R. and Nielsen, O. V. (2000) Scalar calibration of vector magnetometers. *Meas. Sci. Technol.*, 11, 120-132.

Molland, A.F., Wellicome, J.F., Temarel, P., Cic, J. and Taunton, D.J. (2001) Experimental investigation of the seakeeping characteristics of fast displacement catamarans in head and oblique seas. *Transactions of the Royal Institution of Naval Architects*, 143, 78-97.

Tromans, P. S., Anaturk, A. R., and Hagemeyer, P., “A new model for the kinematics of large ocean waves – application as a design wave,” *Proceedings of 1<sup>st</sup> International Offshore and Polar Engineering Conference*, vol. 3, 1991, pp. 64-71.

Vaganay, J., Aldon, M. and Fournier, A. (1993) Mobile robot attitude estimation by fusion of inertial data. *Proc. IEEE Int. Conf. Robotics Automation (ICRA)*, 1, 277-282.

Zimmerman, M. and Sulzer, W. (1991) High bandwidth orientation measurement and control based on complimentary filtering. *Symp. Robotics Control (SYROCO)*, Vienna, Austria.